Heliyon 10 (2024) e37265

Contents lists available at ScienceDirect

Heliyon

journal homepage: www.cell.com/heliyon

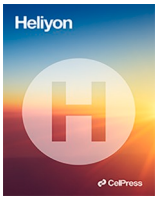

Research article

AHR regulates liver enlargement and regeneration through the YAP signaling pathway

Shenghui Liu

Lin He's Academician Workstation of New Medicine and Clinical Translation, Jining Medical University, Jining, China

ARTICLE INFO

Keywords:
AHR
YAP
Liver enlargement
Liver proliferation

ABSTRACT

The aryl hydrocarbon receptor (AHR) is a transcription factor activated by ligands that participates in many important physiological processes. Although AHR activation is associated with hepatomegaly, the underlying mechanism remains unclear. This study evaluated the effects of AHR activation on liver enlargement and regeneration in various transgenic mice and animal models. Activation of AHR by the non-toxic ligand YH439 significantly induced liver/body weight ratio in wild-type mice (1.37-fold) and $AHR^{fl/fl.ALB\text{-}CreERT2}$ mice (1.54-fold). However, these effects not present in $AHR^{\Delta Hep}$ mice. Additionally, the activation of AHR promotes hepatocyte enlargement (1.43-fold or 1.41-fold) around the central vein (CV) and increases number of $Ki67^{+}$ cells (42.5-fold or 48.8-fold) around the portal vein (PV) in wild-type mice and $AHR^{fl/fl.ALB\text{-}CreERT2}$ mice. In the 70 % partial hepatectomy (PHx) model, YH439 significantly induced hepatocyte enlargement (1.40-fold) and increased number of $Ki67^{+}$ cells (3.97-fold) in $AHR^{fl/fl.ALB\text{-}CreERT2}$ mice. However, these effects were not observed in $AHR^{\Delta Hep}$ mice. Co-immunoprecipitation results suggested a potential protein-protein interaction between AHR and Yes-associated protein (YAP). Disruption of the association between YAP and transcription enhancer domain family member (TEAD) significantly inhibited AHR-induced liver enlargement and regeneration. Furthermore, AHR failed to induce liver enlargement and regeneration in $YAP^{\Delta Hep}$ mice. Blocking the YAP signaling pathway effectively eliminated AHR-induced liver enlargement and regeneration. This study revealed the molecular mechanism of AHR regulation of liver size and regeneration through the activation of AHR-TEAD signaling pathway, thereby offering novel insights into the physiological role of AHR. These findings provide a theoretical foundation for the prevention and treatment of disorders associated with liver regeneration.

1. Introduction

The liver has strong regenerative capacity after injury, and various complex signals are involved in regulating this process [1]. The liver/body weight ratio is consistently regulated during regeneration to maintain a process known as hepatic homeostasis [2]. Many exogenous substances can induce liver enlargement without causing liver damage [3]. However, the molecular mechanisms governing liver size and regeneration are complex and remain elusive.

AHR is a ligand-dependent transcription factor that regulates several physiological processes [4]. AHR is not only involved in the regulation of cytochrome P450 1 (CYP1), an enzyme that metabolizes exogenous compounds [5], but also in many important physiological processes, including cell cycle regulation, cell migration, and cell adhesion [6,7]. AHR exhibits high expression levels in the

E-mail address: 1185553260@qq.com.

https://doi.org/10.1016/j.heliyon.2024.e37265
Received 4 June 2024; Received in revised form 30 July 2024; Accepted 29 August 2024
Available online 2 September 2024

liver and serves as an environmental receptor capable of sensing toxicants and regulating exogenous metabolism [8,9]. 2,3,7,8-Tetrachlorodibenzo-p-dioxin (TCDD) is a prototypical exogenous activator of AHR that is widely used to investigate the toxicological effects associated with this AHR [10]. In hepatotoxicity studies, continuous activation of AHR by TCDD led to cellular hypertrophy, bile duct hyperplasia, steatosis, inflammatory cell infiltration, and transient liver swelling, however, the precise underlying mechanism remains unclear [11]. YH439, an atypical activator of AHR, demonstrates protective properties against liver injury when used as an experimental hepatoprotectant [12]. The differential effects observed between exogenous and endogenous AHR ligands may be attributed to distinct patterns of "sustained" activation by exogenous ligands versus "transient" activation by endogenous ones [8,13].

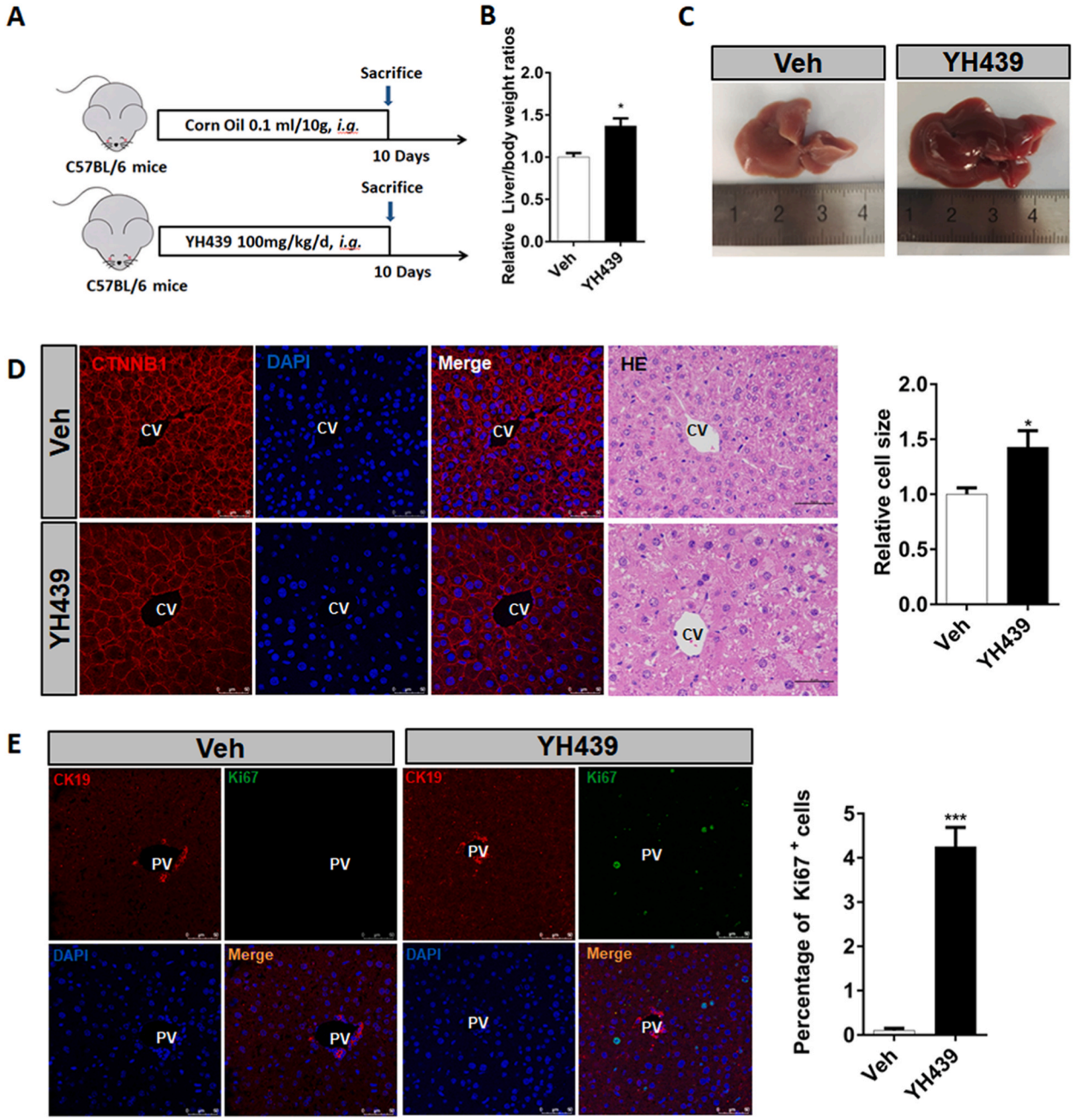

Fig. 1. Activation of AHR promoted liver enlargement and regeneration in wild-type mice. (A) Wild-type mice were treated with vehicle or YH439 (100 mg/kg/d) for 10 days. (B) The relative liver/body weight ratios (n = 5). (C) Representative liver photos of vehicle or YH439-treated mice. (D) CTNNB1 staining, H&E staining were performed to measure the cell size around CV area. Quantification of cell size (n = 5). (E)CK19/Ki67 staining was performed to measure the cell proliferation around PV area. Quantification the number of $Ki67^{+}$ cells (n = 5). Data are expressed as means ± SD; *p < 0.05, **p < 0.01 and ***p < 0.001; Student's t-test. Scale bar = 50 μm.

YAP plays a pivotal role in the regulation of liver size [14,15]. Dephosphorylated YAP translocates from the cytoplasm to the nucleus, and together with TEAD family members, regulates the expression of genes related to liver cell growth, proliferation, and dedifferentiation [16]. The livers of AHR-knockout mice are much smaller than that of wild-type mice [17], suggesting that AHR may also participate in liver size regulation through the YAP signaling pathway. Activation of YAP can induce proliferation and transdifferentiation of mature hepatocytes [16,18]. Previous studies have reported that YAP signal is involved in liver enlargement and liver regeneration induced by the constitutive androstane receptor (CAR), peroxisome proliferators-activated receptorα (PPARα), and pregnane X receptor (PXR) [19–21]. However, the mechanisms underlying the YAP-induced liver enlargement and regeneration require further investigation.

Currently, the relationship between AHR and the YAP signaling pathway remains unclear. It has been observed that TCDD promotes the proliferation of rat hepatocytes (WB-F344) and is associated with the activation of YAP/TAZ (with the PDZ binding motif) transcription targets [22]. In undifferentiated human hepatocytes (HepaRG), TCDD up-regulate the apoptosis suppressor protein

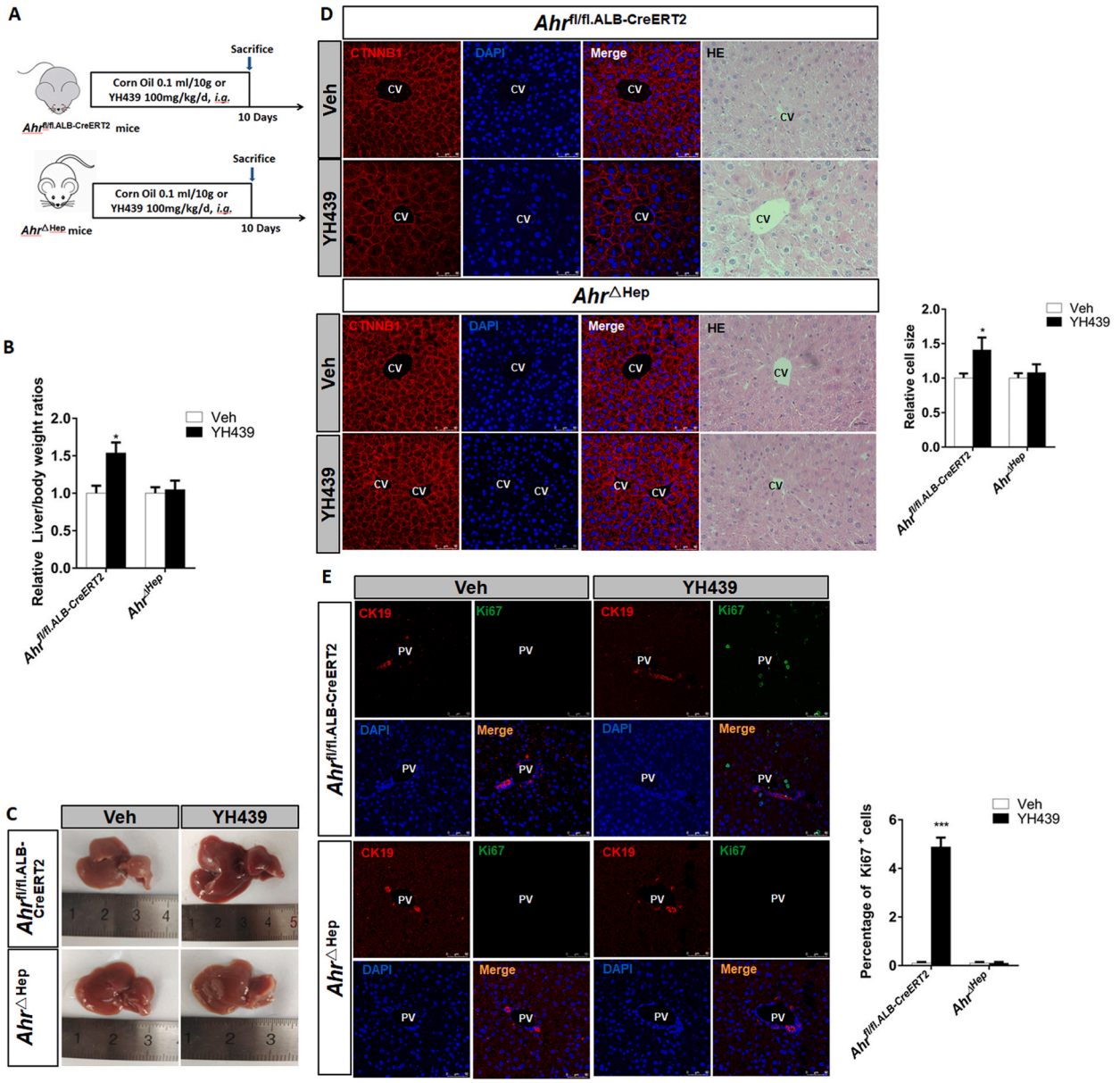

Fig. 2. AHR activation-induced liver enlargement and regeneration is abolished in $Ahr^{\Delta Hep}$mice. (A) $Ahr^{fl/fl.ALB\text{-}CreERT2}$ and $Ahr^{\Delta Hep}$ mice were treated with vehicle or YH439 (100 mg/kg/d) for 10 days. (B) The relative liver/body weight ratios (n = 5). (C) Representative liver photos of vehicle or YH439-treated mice. (D) CTNNB1 staining, H&E staining were performed to measure the cell size around CV area. Quantification of cell size (n = 5). (E)CK19/Ki67 staining was performed to measure the cell proliferation around PV area. Quantification the number of $Ki67^{+}$ cells (n = 5). Data are expressed as means ± SD; *p < 0.05, **p < 0.01 and ***p < 0.001; Student's t-test. Scale bar = 50 μm.

(survivin), a target gene of YAP, and promote cell proliferation [23]. The promotion of hepatocyte proliferation by TCDD may be related to the activation of the YAP signaling pathway. Furthermore, TCDD induced the expression of YAP target gene connective tissue growth factor (CTGF) in rat liver progenitor cells [24]. However, these findings have not been confirmed in vivo. A study found that liver progenitor cells located around the portal vein simultaneously express the sex determining region Y-box transcription factor 9 (SOX9) and hepatocyte nuclear factor 4α (HNF4α). Liver progenitor cells ($SOX9^+$ hepatocyte) can proliferate and differentiate into hepatocytes to repair the liver damage [25]. The in vivo effects of AHR on liver progenitor cells require further investigation.

The objective of this study was to investigate the role of AHR in hepatic hypertrophy and to elucidate its mechanism of action. This study revealed a novel mechanism by which AHR induces liver enlargement and regeneration through the YAP-TEAD signaling pathway, offering new insights into the physiological function of AHR and providing a theoretical foundation for the prevention or treatment of disorders related to liver regeneration.

2. Results

2.1. AHR activation promotes liver enlargement

To investigate the impact of AHR activation on liver enlargement in mice, male C57BL/6 mice were orally administered the AHR-specific agonist YH439 (100 mg/kg/d) for 10 days (Fig. 1A). Subsequently, an increase in the liver/body weight ratio (1.37-fold versus vehicle group, $P < 0.05$) and liver size were observed in YH439-treated mice (Fig. 1B and C). After YH439 treatment, the expression level of AHR target gene cytochrome P450 1A (*Cyp1a1*) was increased in liver (Fig. S1A), the expression levels of proliferation-related genes cyclin A1 (*Ccna1*) and cyclin D1 (*Ccnd1*) were increased (Fig. S1A), and the expression levels of YAP downstream target genes connective tissue growth factor (*Ctgf*), cysteine-rich angiogenic inducer 61 (*Cyr61*) and ankyrin repeat domain 1(*Ankrd1*) were increased (Fig. S1B). However, the expression of inflammatory genes interleukin (*Il-6*), interferon (*Ifn-γ*) and tumor necrosis factor (*Tnfα*) did not change (Fig. S1C).These findings suggest that AHR activation promotes hepatocyte proliferation and induces the activation of the YAP signaling pathway without inducing significant inflammatory damage. Furthermore, biochemical markers related to liver function, such as alanine aminotransferase (ALT), aspartate transaminase (AST), and alkaline phosphatase (ALP), were not significantly altered when compared to the vehicle group (Fig. S1D). This suggests that AHR-induced liver enlargement in mice is not attributable to liver injury but rather a consequence of liver enlargement.

To investigate the effect of AHR activation on hepatocyte size, immunofluorescence catenin β 1 (CTNNB1) staining and hematoxylin-eosin (H&E) staining was performed. YH439 significantly induced hepatocyte enlargement around the CV (1.43-fold versus the vehicle group, $P < 0.05$; Fig. 1D), whereas the size of the hepatocytes around the PV did not increase after YH439 treatment (Fig. S2A), indicating distinct zonal differences in YH439-induced hepatocyte enlargement. To further explore the effect of AHR activation on hepatocyte proliferation, we examined the expression of the cell proliferating nuclear antigen (Ki67) and cytokeratin 19 (CK19) using immunofluorescence. CK19 was used to label bile duct cells around PV. Notably, YH439 treatment significantly increased the number of $Ki67^+$ cells around the PV (42.5-fold versus the vehicle group, $P < 0.001$; Fig. 1E), However, no $Ki67^+$ cells were observed around the CV (Fig. S2B).

$AHR^{fl/fl.ALB\text{-}CreERT2}$ and $AHR^{\Delta Hep}$ mice were orally administered YH439 for 10 days (Fig. 2A). YH439 significantly increased the liver/body weight ratio (1.54-fold versus vehicle group, $P < 0.05$) and liver size in $AHR^{fl/fl.ALB\text{-}CreERT2}$ mice, whereas no changes were observed in $AHR^{\Delta Hep}$ mice (Fig. 2B and C). Administration of YH439 induced notable hepatocyte enlargement around the CV (1.41-fold versus the vehicle group, $P < 0.05$) and increased the number of $Ki67^+$ cells around the PV (48.8-fold versus the vehicle group, $P < 0.001$) in $AHR^{fl/fl.ALB\text{-}CreERT2}$ mice (Fig. 2D and E); however, these effects were not observed in $AHR^{\Delta Hep}$ mice (Figs. S3A and S3B). Furthermore, there was no evident hepatocyte enlargement around the PV or proliferation of hepatocytes around the CV after YH439 treatment in $AHR^{fl/fl.ALB\text{-}CreERT2}$ and $AHR^{\Delta Hep}$ mice. These results show that AHR may promote liver enlargement by facilitating hepatocyte enlargement specifically around the CV and by promoting hepatocyte proliferation specifically around the PV.

2.2. AHR activation promotes liver regeneration

We demonstrated the crucial role of AHR in liver regeneration following 70 % PHx. To determine the effect of AHR activation on liver regeneration, the $AHR^{fl/fl.ALB\text{-}CreERT2}$ and $AHR^{\Delta Hep}$ mice were orally administered YH439 for 2 days after 70 % PHx (Fig. 3A). Hepatocyte size in WT mice was quantified using immunofluorescence CTNNB1 staining and H&E staining. CTNNB1 and H&E staining revealed an increase in hepatocyte size around the CV (1.40-fold versus the vehicle group, $P < 0.05$) in $AHR^{fl/fl.ALB\text{-}CreERT2}$ mice after treatment with YH439, whereas no such effect was observed in $AHR^{\Delta Hep}$ mice (Fig. 3B). YH439 treatment significantly increased the number of $Ki67^+$ cells around the PV (3.97-fold versus the vehicle group, $P < 0.05$) in $AHR^{fl/fl.ALB\text{-}CreERT2}$ mice, which was absent in $AHR^{\Delta Hep}$ mice (Fig. 3C).

Next, we examined specific cell types involved in AHR-induced liver enlargement. Analysis of CK19/Ki67 staining revealed that treatment with YH439 significantly increased the number of $Ki67^+$ cells around the PV(3.97-fold versus the vehicle group, $P < 0.05$) in the $AHR^{fl/fl.ALB\text{-}CreERT2}$ mice; however, no co-staining of CK19 and Ki67 was observed(Fig. 3C), indicating that YH439 did not induce bile duct cell proliferation. SOX9 is expressed in bile duct cells and $SOX9^+$ hepatocytes. Analysis of SOX9/Ki67 staining showed an increased number of SOX9/Ki67 positive cells around the PV (58.2-fold versus the vehicle group, $P < 0.001$) in $AHR^{fl/fl.ALB\text{-}CreERT2}$ mice treated with YH439, whereas YH439 failed to increase this population in $AHR^{\Delta Hep}$ mice (Fig. 4A). These results suggest that YH439 specifically promotes the proliferation of $SOX9^+$ cells. To further confirm this effect on hepatocytes expressing both SOX9 and HNF4α, analysis using SOX9/HNF4α staining demonstrated a significant increase in the number of SOX9/HNF4α positive cells around the PV

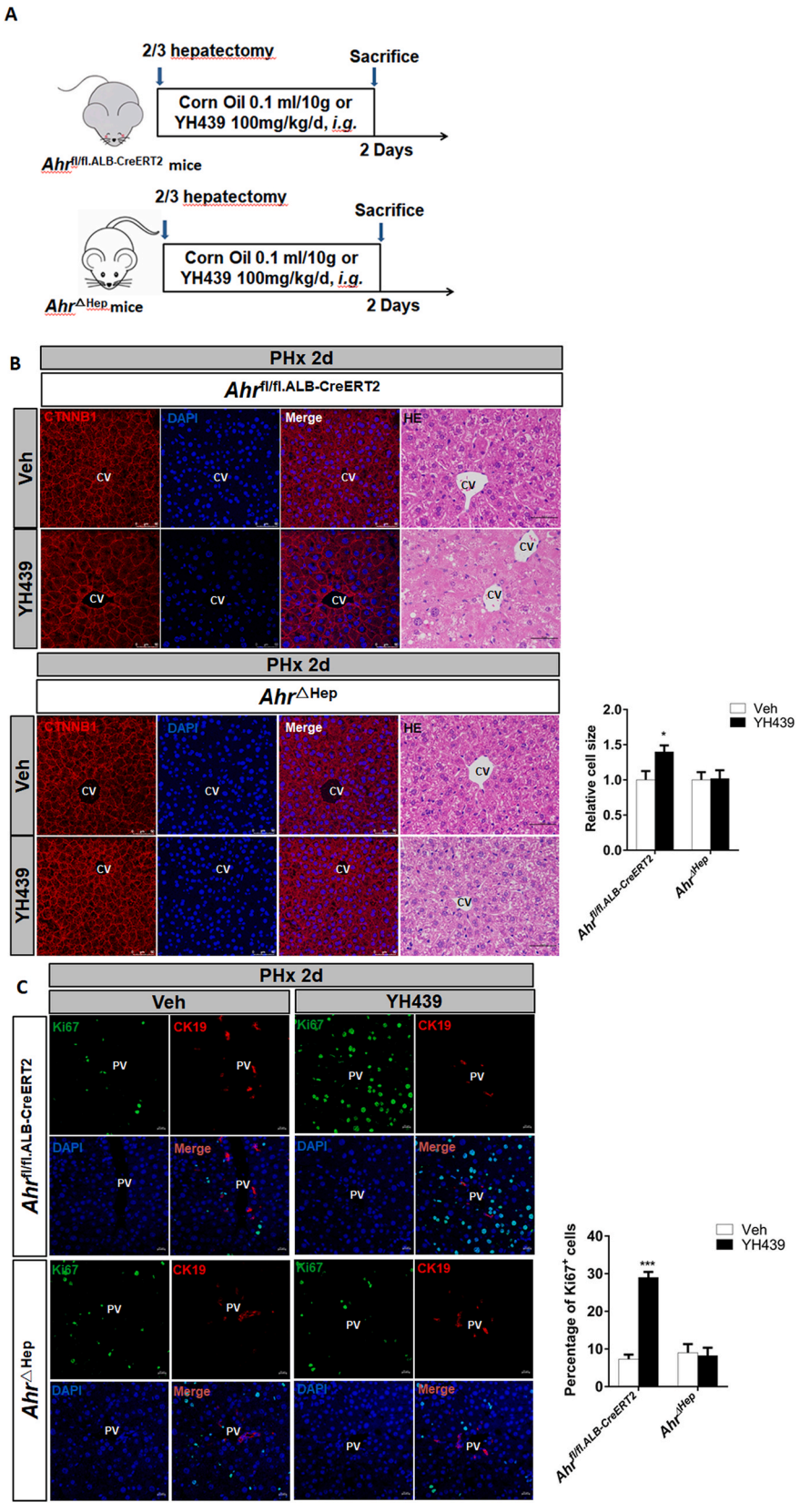

(caption on next page)

Fig. 3. AHR activation promotes liver regeneration (A) *Ahr* $^{fl/fl.ALB\text{-}CreERT2}$ and *Ahr*$^{\Delta Hep}$ mice were treated with vehicle or YH439 (100 mg/kg/d) for 2 days following PHx. (B) (B) CTNNB1 staining, H&E staining were performed to measure the cell size around CV area. Quantification of cell size (n = 5). Scale bar = 50 μm. (C)CK19/Ki67 staining was performed to measure the cell proliferation around PV area. Quantification the number of Ki67^{+} cells (n = 5). Scale bar = 20 μm. Data are expressed as means ± SD; *p < 0.05 and **p < 0.01; Student's t-test.

(28.5-fold versus the vehicle group, P < 0.001) in AHR$^{fl/fl.ALB\text{-}CreERT2}$ mice following treatment with YH439. However, no such increase was observed in AHR$^{\Delta Hep}$ mice (Fig. 4B). These results suggest that AHR promotes liver proliferation by inducing the proliferation of SOX9^{+} hepatocytes around the PV.

2.3. YAP pathway is involved in AHR activation-induced liver enlargement and regeneration

We examined the effect of AHR activation on the YAP signaling pathway. After YH439 treatment, the expression levels of the AHR target gene *Cyp1a1* and the proliferation-related genes *Ccna1* and *Ccnd1* increased in the livers of AHR$^{fl/fl.ALB\text{-}CreERT2}$ mice with 70 % PHx (Fig. 5A), and the expression levels of the downstream YAP target genes *Ctgf, Cyr61* and *Ankrd1* increased (Fig. 5B). These changes were not observed in AHR$^{\Delta Hep}$ mice with 70 % PHx. Compared with the vehicle group, ALT, AST, and ALP levels of AHR$^{fl/fl.ALB\text{-}CreERT2}$ and AHR$^{\Delta Hep}$ mice were not significantly altered (Fig. 5C). These findings suggest that during liver enlargement and regeneration induced by YH439, AHR may have a similar regulatory effect on the YAP signaling pathway. Colocalization experiments demonstrated that treatment with YH439 resulted in the translocation of YAP from the cytoplasm to the nucleus (Fig. 5D). Co-immunoprecipitation experiments confirmed the potential interaction between AHR and YAP (Fig. 5E). These results suggest a protein-protein interaction between AHR and YAP.

2.4. YAP-TEAD interaction is involved in AHR activation-induced liver enlargement and regeneration

YAP functions as a transcriptional coactivator and primarily interacts with TEAD in the nucleus. We further examined whether AHR agonists could induce liver enlargement and regeneration by inhibiting the interaction between YAP and TEAD (Fig. 6A). Verteporfin, an inhibitor of the YAP-TEAD interaction, effectively suppressed the AHR-induced increase in the liver/body weight ratio and liver enlargement (Fig. 6B and C). Furthermore, Verteporfin significantly inhibited hepatocyte enlargement around the CV and hepatocyte proliferation around the PV induced by YH439 (Fig. 6D and E), indicating that the YAP-TEAD interaction is essential for AHR activation-mediated liver enlargement and regeneration.

2.5. AHR-induced liver enlargement and regeneration is YAP dependent

Next, we used YAP$^{fl/fl.ALB\text{-}CreERT2}$ and YAP$^{\Delta Hep}$ mouse models to investigate the role of YAP in AHR-induced liver enlargement and regeneration (Fig. 7A). YH439 increased the liver/body weight ratio (1.51-fold versus the vehicle group, P < 0.05) and liver size in YAP$^{fl/fl.ALB\text{-}CreERT2}$ mice, but failed to increase liver/body weight ratio and liver size in YAP$^{\Delta Hep}$ mice (Fig. 7B and C). Administration of YH439 induced hepatocyte enlargement around the CV (1.41-fold versus the vehicle group, P < 0.05) and increased the number of Ki67^{+} cells around the PV(47.8-fold versus vehicle group, P < 0.001) in YAP$^{fl/fl.ALB\text{-}CreERT2}$ mice, but these effects were not observed in YAP$^{\Delta Hep}$ mice (Fig. 7D and E). Collectively, these findings suggest that both AHR-induced liver enlargement and regeneration are dependent on the YAP signaling pathway.

3. Discussion

The liver possesses a remarkable regenerative capacity following toxin-induced injury or surgical resection [26]; however, the molecular mechanisms governing liver size regulation and regeneration remain. Clarifying these mechanisms is of great significance for the treatment of diseases such as liver regeneration disorders. Our findings demonstrated that the activation of AHR by the non-toxic ligand YH439 induced liver enlargement and regeneration by promoting hepatocyte enlargement around the CV and hepatocyte proliferation around the PV. Moreover, the activation of AHR promoted the translocation of YAP from the cytoplasmic heterotopic region to the nucleus and promoted the activation of YAP downstream target genes. These findings demonstrated that YH439 activated AHR to promote hepatocyte enlargement around the CV and hepatocyte proliferation around the PV through the YAP-TEAD signaling pathway, ultimately inducing liver enlargement and regeneration. In vitro and in vivo experiments, showed that the non-toxic ligand YH439 promoted liver enlargement and regeneration by activating AHR and elucidated its potential molecular mechanism. This study provides a theoretical basis for the prevention or treatment of diseases such as liver regeneration disorders.

Different ligands can trigger distinct pathological or physiological processes via AHR [27]. TCDD activates the AHR and induces various forms of liver damage, thereby contributing to the development of liver cancer [28]. Our findings demonstrate that the non-toxic ligand YH439 activated AHR, promoting hepatocyte enlargement around the CV and hepatocyte proliferation around the PV, thereby inducing liver enlargement and regeneration. The pathways associated with AHR regulation seem to depend on the exposure pattern and persistence of the ligand (acute versus chronic activation or persistent versus non-persistent).Future studies should focus on analyzing the effects of non-toxic endogenous ligands that activate AHR in the liver, while developing non-toxic AHR agonists that may have a positive impact on preventing or treating diseases related to liver regeneration.

Some studies have reported that TCDD inhibited liver regeneration after partial hepatectomy [29]. We discovered that the

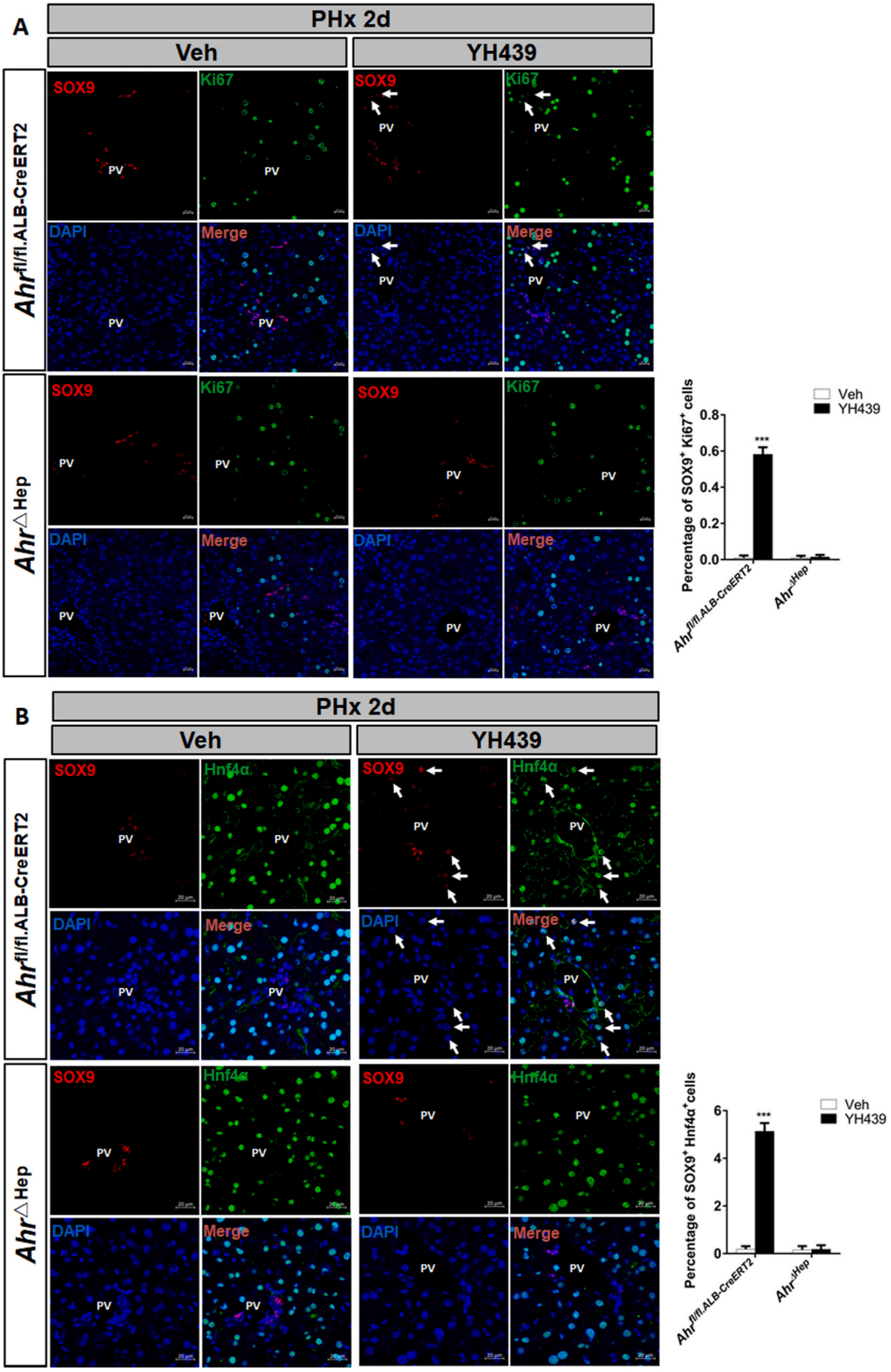

(caption on next page)

Fig. 4. AHR activation induces proliferation of SOX9$^+$ hepatocytes. (A)SOX9/Ki67 staining around PV areas. Quantification the number of SOX9/Ki67$^+$ cells (n = 5). (B) SOX9/HNF4α staining around PV areas. Quantification the number of SOX9/HNF4α$^+$ cells (n = 5). Data are expressed as means ± SD; *p < 0.05, **p < 0.01 and ***p < 0.001; Student's t-test. Scale bar = 20 μm.

non-toxic ligand YH439 promoted hepatocyte enlargement around the CV and proliferation around the PV after partial hepatectomy through AHR activation, thereby inducing liver enlargement and regeneration. These findings demonstrate that the enlargement of hepatocytes around the CV cannot be attributed to an inflammatory response. Furthermore, the current results demonstrated that YH439 did not promote liver regeneration in mice with hepatocellular-specific AHR knockout, suggesting that agonist-induced liver regeneration is mediated by AHR activation in hepatocytes rather than in non-parenchymal cells. This study revealed that AHR induces liver enlargement and regeneration, and accelerates the recovery of liver weight after PHx. All the mice used in this study were male. Further research is required to determine whether the conclusions obtained are sex specific.

The size and quality of the liver are tightly regulated, and multiple types of liver cells are involved in this process. Liver stem cells/progenitor cells play a crucial role in the generation of hepatocytes and bile duct cells [30]. In the case of persistent and severe liver injury, some hepatocytes dedifferentiate into liver stem/progenitor cells to promote regeneration [31]. This study demonstrated that non-toxic YH439 activation of AHR promoted the proliferation of SOX9$^+$ hepatocytes around the PV. There were significant regional differences in the proliferation and enlargement of the AHR-induced hepatocytes. SOX9$^+$ hepatocytes around the PV possess the ability to proliferate and differentiate into hepatocytes [32]. Newborn hepatocytes migrate slowly along the PV-CV axis, which may be an important reason for the hepatocyte regeneration observed around the PV. AHR can be activated by many exogenous compounds [5]. Hepatocytes enlargement shows a zonated distribution responding to specific xenobiotics [33]. In addition, the enzymes involved in enzymes glycolysis, glycogen synthesis, ketogenesis, lipogenesis, and detoxification are mainly located in the CV region [33]. This may explain why hepatocytes enlargement caused by AHR activation occurs mainly around the CV.

The YAP signaling pathway plays a crucial role in regulating organ size and tissue growth, as well as promoting hepatocyte proliferation, and dedifferentiation [34,35]. Using YAP-knockout mice in this study, we demonstrated the indispensable role of the YAP signaling pathway in AHR-induced liver enlargement and regeneration. Furthermore, these findings highlight the importance of YAP-TEAD interaction in AHR-induced liver enlargement and regeneration. Additionally, we identified that the protein-protein interaction between AHR and YAP is also pivotal for liver enlargement and regeneration. However, further investigation is required to precisely determine the specific binding sites and measure the binding affinity between AHR and YAP.

Activation of AHR has a wide range of biological and physiological implications. Therefore, it is crucial to gain a comprehensive understanding of the biological and physiological characteristics and functions of AHR. In summary, this study provides evidence that AHR activation promotes hepatocyte enlargement around the CV and hepatocyte proliferation around the PV through the YAP-TEAD signaling pathway, thereby inducing liver enlargement and regeneration. These results contribute to our understanding of the physiological role of AHR, while also emphasizing its potential in regulating liver size and promoting liver regeneration. Furthermore, these findings provide compelling evidence for AHR as a promising therapeutic target for enhancing liver development and facilitating repair.

Funding information

This work was supported by the medical health science and technology project of Shandong Province no. 202302050527.

Data availability statement

All data produced or analyzed for this study are included in this published article and its supplementary information files. This paper did not report original code. Any additional information required to reanalyze the data reported in this paper is available from the corresponding author.

CRediT authorship contribution statement

Shenghui Liu: Writing – review & editing, Writing – original draft, Project administration, Methodology.

Declaration of competing interest

The authors declare that they have no known competing financial interests or personal relationships that could have appeared to influence the work reported in this paper.

STAR methods

Resource availability

Lead contact. Further information and requests for resources and reagents should be directed to and will be fulfilled by the lead contact, shenghui liu (1185553260@qq.com).

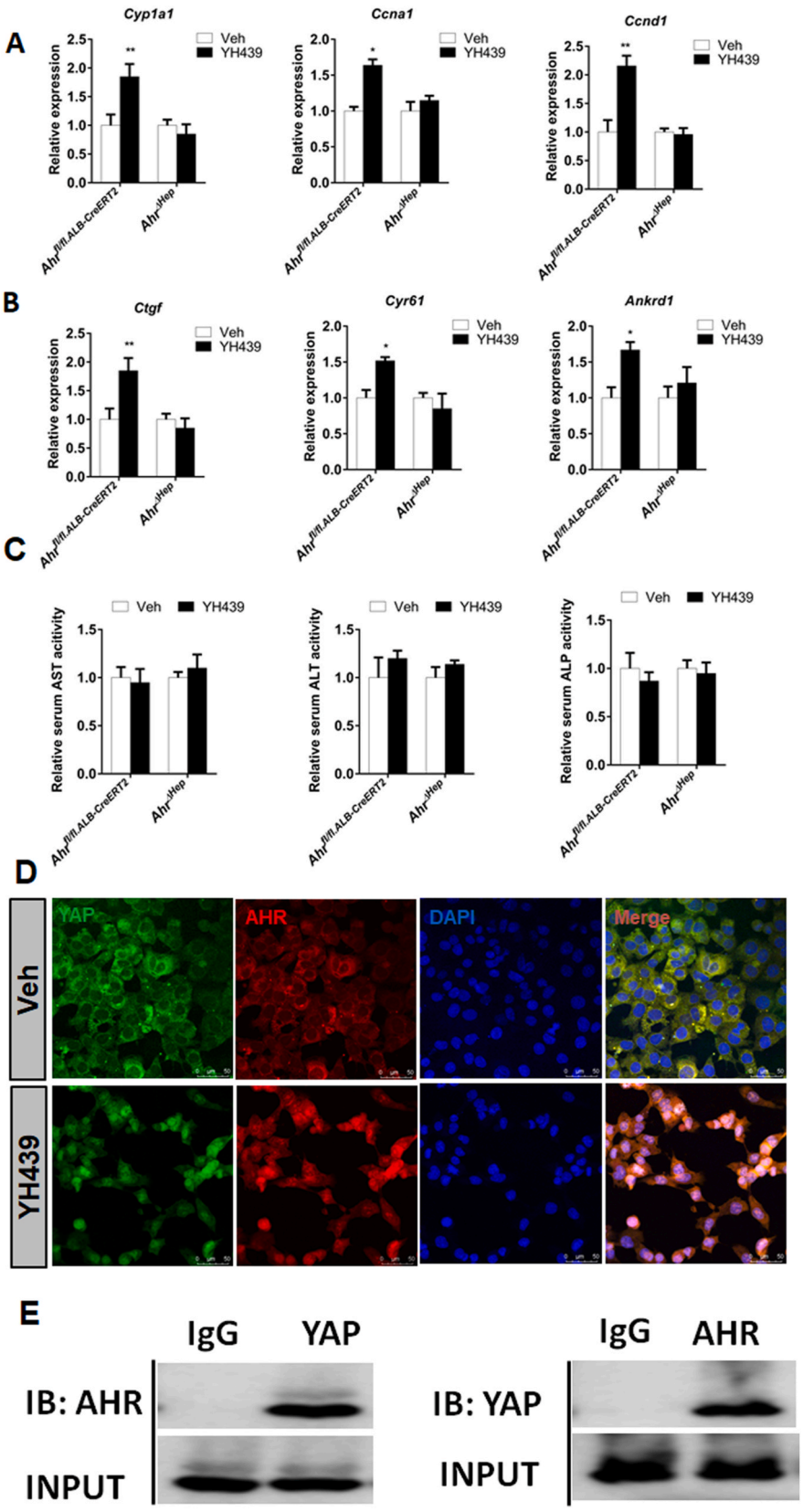

(caption on next page)

Fig. 5. AHR regulates YAP signaling pathway. (A) Qpcr analysis of AHR downstream gene, and proliferation-related genes in PHx mice (n = 5). (B) Qpcr analysis of YAP downstream gene in PHx mice (n = 5). (C) Serum AST, ALT and ALP levels after YH439 treatment in PHx mice (n = 5). (D) Immunofluorescence staining of AHR and YAP in Primary Mouse Hepatocytes treated with 5 μM of YH439 for 48 h. Nuclei were counterstained with DAPI. (E) Co-IP of AHR and YAP to assess their protein-protein interaction in primary hepatocyte extracts. Data are expressed as means ± SD; *p < 0.05 and **p < 0.01; Student's t-test.

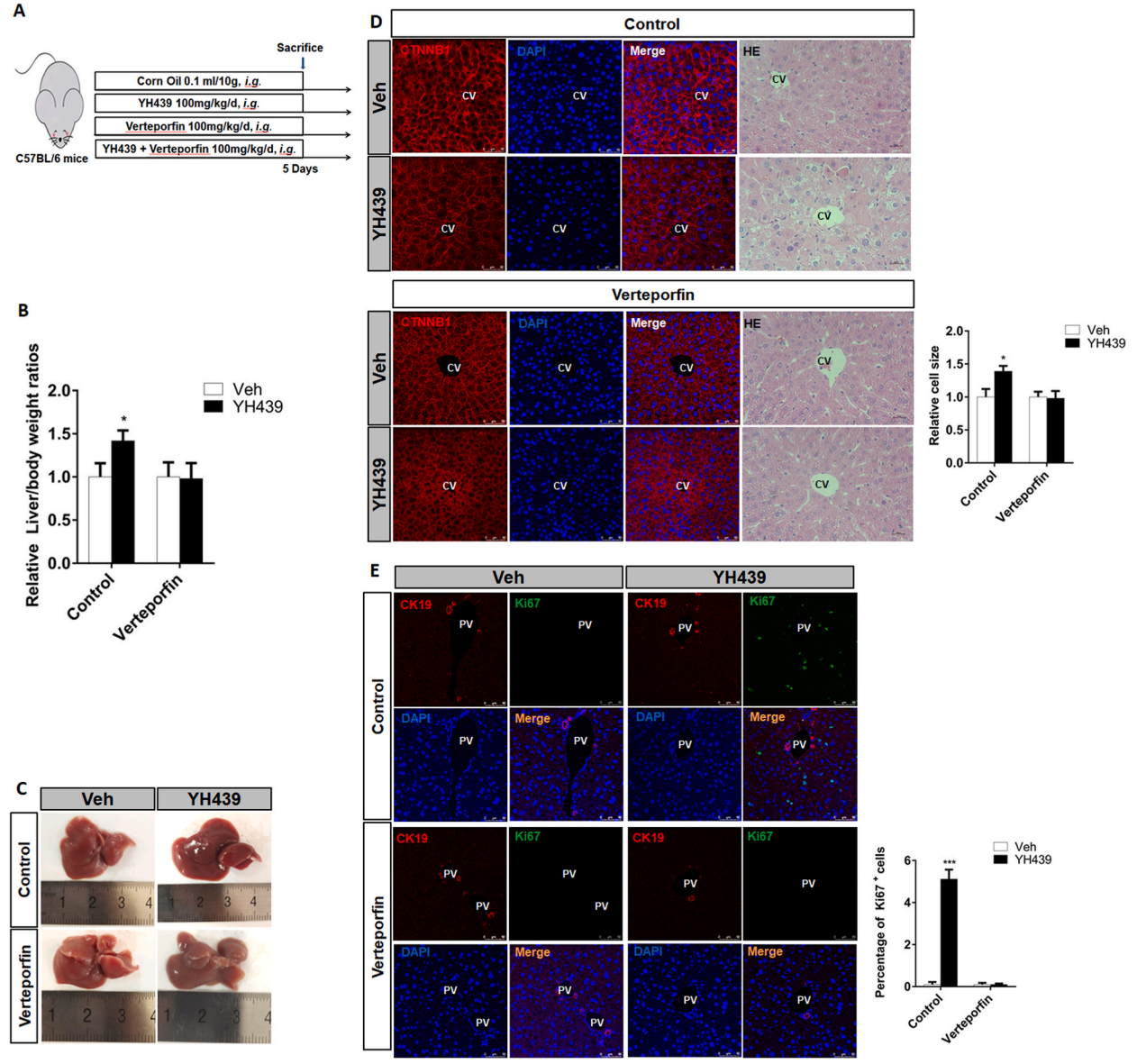

Fig. 6. YAP-TEAD interaction is involved in AHR-induced liver enlargement and regeneration. (A) Corn oil-treated mice and verteporfin-treated mice were administered vehicle or YH439 (100 mg/kg/d) for 5 days. (B) The relative liver/body weight ratios (n = 5). (C) Representative liver photos of vehicle or YH439-treated mice. (D) CTNNB1 staining, H&E staining were performed to measure the cell size around CV area. Quantification of cell size (n = 5). (E)CK19/Ki67 staining were performed to measure the cell proliferation around PV area. Quantification the number of $Ki67^+$ cells (n = 5). Data are expressed as means ± SD; *p < 0.05, **p < 0.01 and ***p < 0.001; Student's t-test. Scale bar = 50 μm.

Materials availability. This study did not generate new unique materials.

Data and code availability. All data produced or analyzed for this study are included in this published article and its supplementary information files. This paper did not report original code. Any additional information required to reanalyze the data reported in this paper is available from the lead contact upon request.

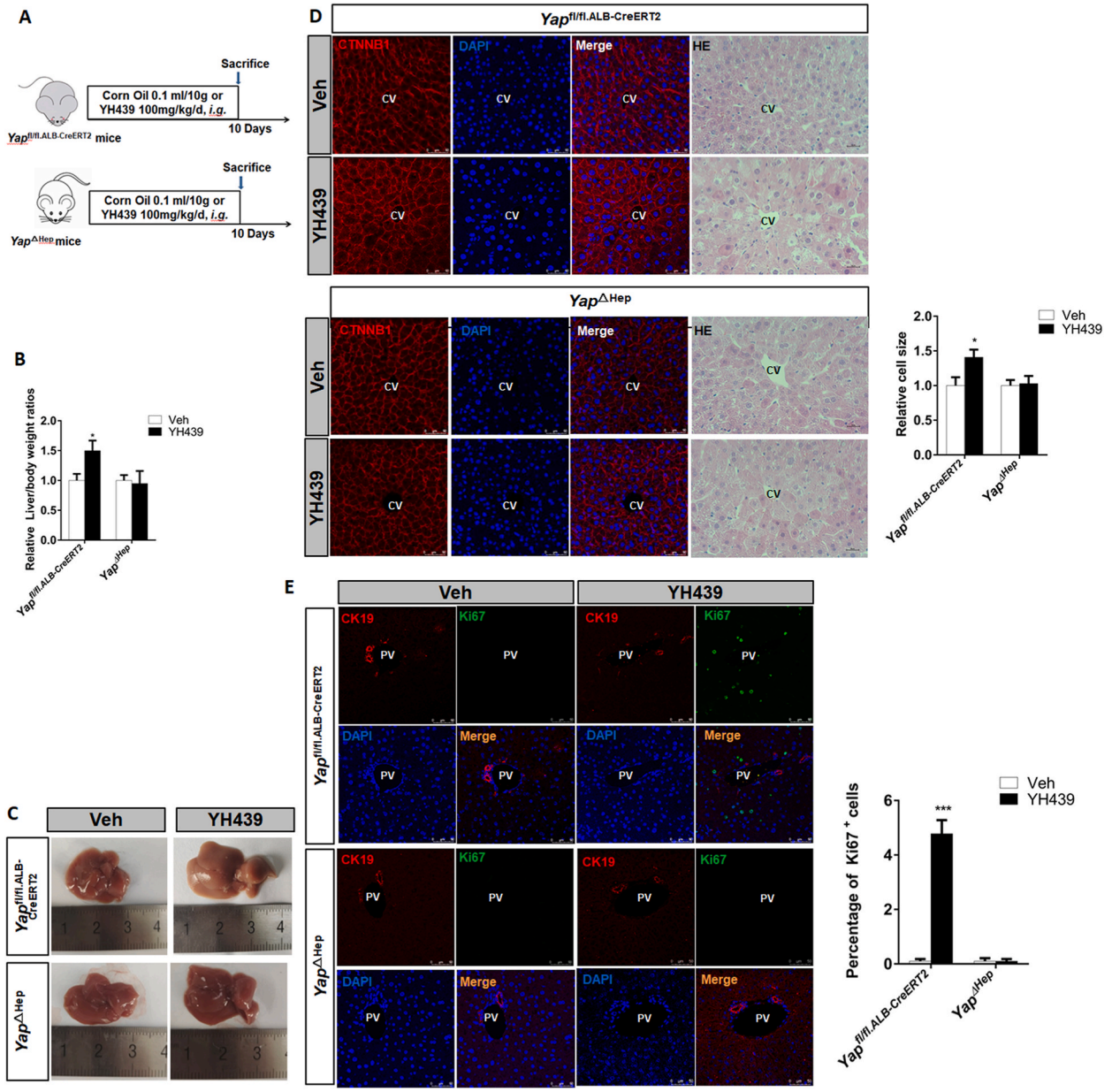

Fig. 7. Yap is involved in AHR-induced liver enlargement and regeneration. (A) *Yap*$^{fl/fl.ALB\text{-}CreERT2}$ and *Yap*$^{\Delta Hep}$ were treated with vehicle or YH439 (100 mg/kg/d) for 10 days. (B) The relative liver/body weight ratios (n = 5). (C) Representative liver photos of vehicle or YH439-treated mice. (D) CTNNB1 staining, H&E staining were performed to measure the cell size around CV area. Quantification of cell size (n = 5). (E)CK19/Ki67 staining was performed to measure the cell proliferation around PV area. Quantification the number of Ki67^{+} cells (n = 5). Data are expressed as means ± SD; *p < 0.05, **p < 0.01 and ***p < 0.001; Student's t-test. Scale bar = 50 μm.

Experimental model and subject details

Animal studies

The wild-type (WT) mice were obtained from Jinan Pengyue Experimental Animal Breeding Co., Ltd (Jinan, China) and against a C57BL6/J background. AHR$^{fl/fl}$ mice (B6.129(Cg)-Ahrem1Bra/J, stock number 035734), YAP$^{fl/fl}$ mice(B6.129P2(Cg)-Yap1tm1.1Dupa/J, stock number 032192) were obtained from the Jackson Laboratory. ALB-Cre^{ERT2} mice (B6.129S-Albtm1.1 (CreERT2)Smoc, stock number NM-KI-00002) were obtained from the Shanghai Model Organisms Center, Inc(Shanghai, China). AHR$^{fl/fl}$ mice or YAP$^{fl/fl}$ mice were crossed with ALB-Cre^{ERT2} mice to obtain AHR$^{fl/fl}$; ALB-Cre^{ERT2} heterozygous mice (AHR$^{fl/fl.ALB\text{-}CreERT2}$ mice) or YAP$^{fl/fl}$; ALB-Cre^{ERT2} heterozygous mice (YAP $^{fl/fl.ALB\text{-}CreERT2}$ mice). These heterozygous mice were intraperitoneally injected with tamoxifen (Sigma, T5648, 100 mg/kg/d) for three days to obtain hepatocyte-specific AHR-deficient mice (AHR$^{\Delta Hep}$

mice) or hepatocyte-specific YAP-deficient mice ($YAP^{\Delta Hep}$ mice). Tamoxifen was dissolved in corn oil. The wild-type (WT) mice, $AHR^{fl/fl.ALB\text{-}CreERT2}$ mice, $AHR^{\Delta Hep}$ mice, $YAP^{fl/fl.ALB\text{-}CreERT2}$ mice or $YAP^{\Delta Hep}$ were 6–8 week-old in this study (male, n = 5 per group). These mice were orally treated with Vehicle (Corn Oil 0.1 ml/10g) or YH439 (MCE, HY-100242, 100 mg/kg/d) [36]for ten days. $AHR^{fl/fl.ALB\text{-}CreERT2}$ mice and $AHR^{\Delta Hep}$ mice after partial hepatectomy orally treated with Vehicle or YH439 for two days. The WT mice were orally treated with Vehicle, YH439, Verteporfin (MCE, HY-B0146, 100 mg/kg/d) [20] or Verteporfin + YH439 for ten days. We used the doses of YH439 and Vertepofen based on previous research [20,36]. $YAP^{fl/fl.ALB\text{-}CreERT2}$ mice, $YAP^{\Delta Hep}$ mice were orally treated with Vehicle, YH439 for ten days. The mice were euthanized under anesthesia (exposed to CO_2 gradual fill in a chamber with a displacement rate of 30 % chamber volume per minute), liver tissue was cryopreserved using liquid nitrogen or fixed in 10 % formalin buffer solution, followed by embedding in paraffin or OCT compound. Additionally, serum samples were collected. All experimental procedures were conducted in accordance with the Experimental Animal Ethics Committee of Jining Medical College (Ethics approval number: JNMC-2023-DW-158). The entire study adhered to the principles of Replacement, Reduction, and Refinement (3Rs) for animal experiments and was performed under the guidance of respecting the ARRIVE criteria [37].

Isolation of primary mouse hepatocytes

Wild mice were used to isolate primary hepatocytes, the separation procedure described in our previous study [32].

RNA isolation and QRT-PCR

The experimental procedure was described in our previous study [32]. The RNAiso Plus (Takara, Cat#9109) was used to extract total RNA from the liver. Then PrimeScript RT Reagent Kit with gDNA Eraser (Takara, Cat#RR047A) was used for the synthesis of cDNA. The ChamQ SYBR Color qPCR Master Mix (Low ROX Premixed) is utilized for real-time PCR analysis. The comparative-Ct method ($2^{-\triangle\triangle Ct}$ method) was used to calculate the relative level. All sequence of primers was listed in Table S1.

Serum transaminase levels and histological analysis

Plasma ALT, AST and ALP were analyzed with GPT/ALT kit (Nanjing jiancheng, Cat#C009-2)and GOT/AST kit (Nanjing jiancheng, C010-2) or Alkaline Phosphatase Assay kit (Beyotime, Cat#P0321S),respectively. The handling of liver samples was described in our previous study [32], and H&E staining kit (Beyotime, Cat#C0105S) was used for H&E staining.

Immunofluorescent analysis

The experimental procedure was described in our previous study [32]**.** For cell immunofluorescent staining, Anti-YAP (1:100 dilution, Proteintech, Cat# 66900-1-Ig, RRID: AB_2882229), Anti-AHR (1:100 dilution, BOSTER Cat# A00225-4, RRID: AB_3095576) were used as primary antibody. DyLight 488 Conjugated AffiniPure Goat Anti-mouse IgG (H + L) (1:500 dilution, BOSTER Cat# BA1126, RRID: AB_2827694) and DyLight 594 Conjugated AffiniPure Goat Anti-rabbit IgG (H + L) (1:500 dilution, BOSTER Cat# BA1142, RRID: AB_3095580) were used as secondary antibodies. DAPI (Abcam, Cat# ab104139) staining the nucleus. For immunohistochemical staining, Anti-Ki67 (1:100 dilution, BOSTER, Cat# M00254-8, RRID: AB_3081764), Anti-CTNNB1(1:100 dilution BOSTER, Cat#PA1212, RRID:AB_3082601), Anti-CK19(1:100 dilution BOSTER, Cat#PB9715, RRID:AB_3082234)/Anti- Ki67 (1:100 dilution), CTNNB1(1:100 dilution)/Ki67(1:100 dilution), Anti-Sox9(1:100 dilution BOSTER, Cat#BM4268, RRID: AB_2941988)/Anti-Ki67 (1:100 dilution), Anti-Sox9(1:100 dilution)/Anti- Ki67 (1:100 dilution), Anti-Sox9(1:100 dilution)/Anti-HNF4α (1:100 dilution, Santa Cat#sc-374229, RRID:AB_10989766) were used as primary antibody. DyLight 488 Conjugated AffiniPure Goat Anti-mouse IgG (H + L) (1:500 dilution) and DyLight 594 Conjugated AffiniPure Goat Anti-rabbit IgG (H + L) (1:500 dilution) were used as secondary antibodies. DAPI (Abcam, Cat# ab104139) staining the nucleus. A laser scanning confocal microscope (LEICA, DMI8) was used to capture the images.

Co-immunoprecipitation (Co-IP)

Primary mouse hepatocytes treated with YH439 (5 μM, MCE Cat# HY-100242) for 48 h. Co-IP was conducted using Thermo Scientific Pierce Co-IP kit (Thermo Scientific, Cat# 26149). Experimental product was analyzed by Western blot.

Western blots

The experimental procedure was described in our previous study [32]**.** Anti-AHR (1:200 dilution), anti-YAP (1:500 dilution) were used as primary antibody. HRP-conjugated Affinipure Goat Anti-Mouse IgG(H + L) (1:1000 dilution, Proteintech, Cat# SA00001-1, RRID: AB_2890995) and HRP-conjugated Affinipure Goat Anti-Rabbit IgG(H + L) (1:1000 dilution, Proteintech, Cat# SA00001-2, RRID: AB_2722564) were used as secondary antibodies.

Software–immunofluorescence staining quantification

Image Pro Plus is used to analyze and quantify data in photomicrographs. For CTNNB1, Ki67, HNF4α/SOX9, Ki67/SOX9 staining quantification, the experimental procedure was described in previous study [19]**.** For CTNNB1 staining quantification, the number of hepatocytes was counted by Image Pro Plus, the edges of the central vein (CV) and CV area was measured by Image Pro Plus, and then the area of the whole visual field was measured by Image Pro Plus. After that, the CV area was subtracted from whole visual field and the average area of each hepatocyte was calculated. For, Ki67, HNF4α/SOX9, Ki67/SOX9 staining quantification, the total number of hepatocytes and the number of Ki67, HNF4α/SOX9, and Ki67/SOX9 cells were counted, respectively. And then, the percentage of Ki67 cells was calculated [19]. The number of mice in each experimental group is 5 (n = 5). Each liver randomly selected 3 areas (around the portal vein or around the central vein) to obtain images and their average were plotted and analyzed.

Quantitative and statistical analysis

Statistical analyses were performed using the GraphPad Prism 6 (GraphPad). Data are expressed as means ± SD. Comparisons between two groups were performed using the two-tailed Student's t-test. Comparisons between multiple groups were performed using ordinary one-way ANOVA with the Dunnett's multiple comparison test. Statistical significance was presented at the level of $*p < 0.05$, $**p < 0.01$, $***p < 0.001$.

Appendix A. Supplementary data

Supplementary data to this article can be found online at https://doi.org/10.1016/j.heliyon.2024.e37265.

References

[1] G.K. Michalopoulos, B. Bhushan, Liver regeneration: biological and pathological mechanisms and implications, Nat. Rev. Gastroenterol. Hepatol. 18 (1) (2021) 40–55, https://doi.org/10.1038/s41575-020-0342-4.

[2] G.K. Michalopoulos, Hepatostat: liver regeneration and normal liver tissue maintenance, Hepatology 65 (4) (2017) 1384–1392, https://doi.org/10.1002/hep.28988.

[3] A. Columbano, G.M. Ledda-Columbano, Mitogenesis by ligands of nuclear receptors: an attractive model for the study of the molecular mechanisms implicated in liver growth, Cell Death Differ. 10 (Suppl 1) (2003) S19–S21, https://doi.org/10.1038/sj.cdd.4401113.

[4] C.A. Opitz, P. Holfelder, M.T. Prentzell, S. Trump, The complex biology of aryl hydrocarbon receptor activation in cancer and beyond, Biochem. Pharmacol. 216 (2023) 115798, https://doi.org/10.1016/j.bcp.2023.115798.

[5] A. Braeuning, C. Köhle, A. Buchmann, M. Schwarz, Coordinate regulation of cytochrome P450 1a1 expression in mouse liver by the aryl hydrocarbon receptor and the beta-catenin pathway, Toxicol. Sci. 122 (1) (2011) 16–25, https://doi.org/10.1093/toxsci/kfr080.

[6] J.L. Marlowe, A. Puga, Aryl hydrocarbon receptor, cell cycle regulation, toxicity, and tumorigenesis, J. Cell. Biochem. 96 (6) (2005) 1174–1184, https://doi.org/10.1002/jcb.20656.

[7] T. Kung, K.A. Murphy, L.A. White, The aryl hydrocarbon receptor (AhR) pathway as a regulatory pathway for cell adhesion and matrix metabolism, Biochem. Pharmacol. 77 (4) (2009) 536–546, https://doi.org/10.1016/j.bcp.2008.09.031.

[8] J. Yan, H.C. Tung, S. Li, Y. Niu, W.G. Garbacz, P. Lu, et al., Aryl hydrocarbon receptor signaling prevents activation of hepatic stellate cells and liver fibrogenesis in mice, Gastroenterology 157 (3) (2019) 793–806.e14, https://doi.org/10.1053/j.gastro.2019.05.066.

[9] M.J. Heo, J.H. Suh, S.H. Lee, K.L. Poulsen, Y.A. An, B. Moorthy, et al., Aryl hydrocarbon receptor maintains hepatic mitochondrial homeostasis in mice, Mol. Metabol. 72 (2023) 101717, https://doi.org/10.1016/j.molmet.2023.101717.

[10] S.A. Piwarski, T.B. Salisbury, The effects of environmental aryl hydrocarbon receptor ligands on signaling and cell metabolism in cancer, Biochem. Pharmacol. 216 (2023) 115771, https://doi.org/10.1016/j.bcp.2023.115771.

[11] J. Vondráček, M. Machala, Environmental ligands of the aryl hydrocarbon receptor and their effects in models of adult liver progenitor cells, Stem Cell. Int. 2016 (2016) 4326194, https://doi.org/10.1155/2016/4326194.

[12] E.Y. Choi, S.G. Kim, J.W. Lee, J.K. Yoo, J.K. Shin, N.D. Kim, Suppression of rat hepatic cytochrome P450 2E1 expression by isopropyl 2-(1,3-dithioetane-2-ylidene)-2-[N-(4-methyl-thiazol-2-yl)carbamoyl] acetate (YH439), an experimental hepatoprotectant: protective role against hepatic injury, Biochem. Pharmacol. 52 (8) (1996) 1219–1225, https://doi.org/10.1016/0006-2952(96)00474-1.

[13] L. Stejskalova, Z. Dvorak, P. Pavek, Endogenous and exogenous ligands of aryl hydrocarbon receptor: current state of art, Curr. Drug Metabol. 12 (2) (2011) 198–212, https://doi.org/10.2174/138920011795016818.

[14] X. Li, S. Fan, C. Cai, Y. Gao, X. Wang, Y. Zhang, et al., YAP regulates the liver size during the fasting-refeeding transition in mice, Acta Pharm. Sin. B 13 (4) (2023) 1588–1599, https://doi.org/10.1016/j.apsb.2022.12.011.

[15] S.H. Patel, F.D. Camargo, D. Yimlamai, Hippo signaling in the liver regulates organ size, cell fate, and carcinogenesis, Gastroenterology 152 (3) (2017) 533–545, https://doi.org/10.1053/j.gastro.2016.10.047.

[16] J.O. Russell, F.D. Camargo, Hippo signalling in the liver: role in development, regeneration and disease, Nat. Rev. Gastroenterol. Hepatol. 19 (5) (2022) 297–312, https://doi.org/10.1038/s41575-021-00571-w.

[17] J.A. Harrill, R.R. Hukkanen, M. Lawson, G. Martin, B. Gilger, V. Soldatow, et al., Knockout of the aryl hydrocarbon receptor results in distinct hepatic and renal phenotypes in rats and mice, Toxicol. Appl. Pharmacol. 272 (2) (2013) 503–518, https://doi.org/10.1016/j.taap.2013.06.024.

[18] T. Su, T. Bondar, X. Zhou, C. Zhang, H. He, R. Medzhitov, Two-signal requirement for growth-promoting function of Yap in hepatocytes, Elife 4 (2015) e02948, https://doi.org/10.7554/eLife.02948.

[19] Y. Gao, S. Fan, H. Li, Y. Jiang, X. Yao, S. Zhu, et al., Constitutive androstane receptor induced-hepatomegaly and liver regeneration is partially via yes-associated protein activation, Acta Pharm. Sin. B 11 (3) (2021) 727–737, https://doi.org/10.1016/j.apsb.2020.11.021.

[20] S. Fan, Y. Gao, A. Qu, Y. Jiang, H. Li, G. Xie, et al., YAP-TEAD mediates PPAR α-induced hepatomegaly and liver regeneration in mice, Hepatology 75 (1) (2022) 74–88, https://doi.org/10.1002/hep.32105.

[21] Y. Jiang, D. Feng, X. Ma, S. Fan, Y. Gao, K. Fu, et al., Pregnane X receptor regulates liver size and liver cell fate by yes-associated protein activation in mice, Hepatology 69 (1) (2019) 343–358, https://doi.org/10.1002/hep.30131.

[22] J. Svobodová, M. Kabátková, L. Šmerdová, P. Brenerová, Z. Dvořák, M. Machala, et al., The aryl hydrocarbon receptor-dependent disruption of contact inhibition in rat liver WB-F344 epithelial cells is linked with induction of survivin, but not with inhibition of apoptosis, Toxicology 333 (2015) 37–44, https://doi.org/10.1016/j.tox.2015.04.001.

[23] H. Li, A. Wolfe, S. Septer, G. Edwards, X. Zhong, A.B. Abdulkarim, et al., Deregulation of Hippo kinase signalling in human hepatic malignancies, Liver Int. 32 (1) (2012) 38–47, https://doi.org/10.1111/j.1478-3231.2011.02646.x.

[24] D. Faust, J. Vondráček, P. Krčmář, L. Smerdová, J. Procházková, E. Hrubá, et al., AhR-mediated changes in global gene expression in rat liver progenitor cells, Arch. Toxicol. 87 (4) (2013) 681–698, https://doi.org/10.1007/s00204-012-0979-z.

[25] J. Font-Burgada, S. Shalapour, S. Ramaswamy, B. Hsueh, D. Rossell, A. Umemura, et al., Hybrid periportal hepatocytes regenerate the injured liver without giving rise to cancer, Cell 162 (4) (2015) 766–779, https://doi.org/10.1016/j.cell.2015.07.026.

[26] N. Fausto, Liver regeneration, J. Hepatol. 32 (1 Suppl) (2000) 19–31, https://doi.org/10.1016/s0168-8278(00)80412-2.

[27] J.C. Granados, K. Falah, I. Koo, E.W. Morgan, G.H. Perdew, A.D. Patterson, et al., AHR is a master regulator of diverse pathways in endogenous metabolism, Sci. Rep. 12 (1) (2022) 16625, https://doi.org/10.1038/s41598-022-20572-2.

[28] K.W. Bock, C. Köhle, Ah receptor- and TCDD-mediated liver tumor promotion: clonal selection and expansion of cells evading growth arrest and apoptosis, Biochem. Pharmacol. 69 (10) (2005) 1403–1408, https://doi.org/10.1016/j.bcp.2005.02.004.

[29] D.P. Jackson, H. Li, K.A. Mitchell, A.D. Joshi, C.J. Elferink, Ah receptor-mediated suppression of liver regeneration through NC-XRE-driven p21Cip1 expression, Mol. Pharmacol. 85 (4) (2014) 533–541, https://doi.org/10.1124/mol.113.089730.

[30] A. Miyajima, M. Tanaka, T. Itoh, Stem/progenitor cells in liver development, homeostasis, regeneration, and reprogramming, Cell Stem Cell 14 (5) (2014) 561–574, https://doi.org/10.1016/j.stem.2014.04.010.

[31] K. Furuyama, Y. Kawaguchi, H. Akiyama, M. Horiguchi, S. Kodama, T. Kuhara, et al., Continuous cell supply from a Sox9-expressing progenitor zone in adult liver, exocrine pancreas and intestine, Nat. Genet. 43 (1) (2011) 34–41, https://doi.org/10.1038/ng.722.
[32] S. Liu, D. Qin, Y. Yan, J. Wu, L. Meng, W. Huang, et al., Metabolic nuclear receptors coordinate energy metabolism to regulate Sox9(+) hepatocyte fate, iScience 24 (9) (2021) 103003, https://doi.org/10.1016/j.isci.2021.103003.
[33] T. Kietzmann, Metabolic zonation of the liver: the oxygen gradient revisited, Redox Biol. 11 (2017) 622–630, https://doi.org/10.1016/j.redox.2017.01.012.
[34] Y. Liu, S. Zhuo, Y. Zhou, L. Ma, Z. Sun, X. Wu, et al., Yap-Sox9 signaling determines hepatocyte plasticity and lineage-specific hepatocarcinogenesis, J. Hepatol. 76 (3) (2022) 652–664, https://doi.org/10.1016/j.jhep.2021.11.010.
[35] M. Bou Saleh, A. Louvet, L.C. Ntandja-Wandji, E. Boleslawski, V. Gnemmi, G. Lassailly, et al., Loss of hepatocyte identity following aberrant YAP activation: a key mechanism in alcoholic hepatitis, J. Hepatol. 75 (4) (2021) 912–923, https://doi.org/10.1016/j.jhep.2021.05.041.
[36] F. Whelan, N. Hao, S.G. Furness, M.L. Whitelaw, A. Chapman-Smith, Amino acid substitutions in the aryl hydrocarbon receptor ligand binding domain reveal YH439 as an atypical AhR activator, Mol. Pharmacol. 77 (6) (2010) 1037–1046, https://doi.org/10.1124/mol.109.062927.
[37] A.A. Percie du Sert N, S. Alam, M.T. Avey, M. Baker, W.J. Browne, et al., Reporting Animal Research: Explanation and Elaboration for the ARRIVE Guidelines 2.0, vol. 18, 2020 e3000411, https://doi.org/10.1371/journal.pbio.3000411, 7.